XPS, UV-Vis, FTIR and EXAFS Studies to Investigate the Binding Mechanism of N719 dye onto Oxalic Acid Treated TiO_2 and Its Implication on Photovoltaic Properties

Jaspreet Singh[1], Abhay Gusain[1], Vibha Saxena[1*], A.K. Chauhan[1], P. Veerender[1], S.P. Koiry[1], P.Jha[1], Avani Jain[2], D.K. Aswal[1#] and S.K. Gupta[1]

[1]*Bhabha Atomic Research Centre, Technical Physics Division, Trombay, Mumbai-400 085, India*
[2]*Centre for Converging Technologies, University of Rajsthan, Jaipur-302004, India*

Abstract:

The anchoring mechanism of N719 dye molecules on oxalic acid treated TiO_2 (OA-TiO_2) electrodes has been investigated using extended X-ray absorption fine structure (EXAFS) measurements, Fourier transform infrared spectroscopy (FTIR), UV-Vis spectroscopy and X-ray photoelectron spectroscopy (XPS). The FTIR spectroscopy of OA-TiO_2 electrodes revealed that the oxalic acid dissociates at the TiO_2 surface and binds through bidentate chelating and/or bidentate bridging. Analyses of EXAFS, FTIR, UV-Vis and XPS measurements of N719 dye loaded onto OA-TiO_2 revealed that the binding of N719 molecules takes place via interaction between Ru atom of the dye and O^- of bidentate bridged oxalate ions at TiO_2 surface. This mechanism is quite different to the binding of N719 onto untreated TiO_2 (WO-TiO_2) surface, where -COOH and SCN groups of the dye directly bind to TiO_2 surface. The analyses of UV-Vis data show that the amount of N719 dye loading is much higher onto OA-TiO_2 surface as compared to the native TiO_2 surface. In addition, the incident photon to current conversion efficiency (IPCE) measurements show that presence of oxalate ions between dye and TiO_2 surface favors efficient electron transfer, and therefore, improvement in device efficiency. The dye sensitized solar cells fabricated using N719 dye sensitized onto OA-TiO_2 showed an efficiency of ~4.6%, which is significantly higher than that based on WO-TiO_2 electrode (~3.2%).

Keywords: N719 dye, binding mechanism, EXAF, dye sensitized solar cell

---

To whom correspondence should be addressed.

Electronic Mail:
[1#]dkaswal@yahoo.com,[1*]vibhas@barc.gov.in

1. INTRODUCTION

Dye-sensitized solar cells (DSSCs) are being investigated extensively as potential devices for harnessing solar power owing to ease of fabrication and their relatively low cost as compared to the conventional silicon solar cells[1-3]. Devices with efficiency exceeding 10% has been fabricated using nanoporous TiO_2 sensitized with Ru(II)-polypyridyl complexes, such as N3, N719[4]. It is well established that modification of the TiO_2 surface plays a major role in determining the efficiency of the DSSCs. It has also been demonstrated that the short circuit current (J_{SC}), and therefore, efficiency of the DSSC improves by the treatment of TiO_2 electrode by 0.1M HCl treatment[5]. In addition, other acids such as HNO_3, H_3PO_4 and H_2SO_4 have also been reported to affect the photovoltaic properties and therefore the device efficiency[6-8]. The improvement in efficiency as a result of surface treatment in the DSSCs has been attributed to the negative movement of the TiO_2 conduction band edge (CBE), enhanced dye absorption and reduced charge recombination. In order to understand the improvement in the device performance as a result of surface modifications, it is important to understand the interfacial properties of the materials involved in the fabrication of DSSCs. In general, at TiO_2 semiconductor/dye interface, ultrafast electron injection from the excited dye to the conduction band of the TiO_2 takes place which is responsible for the improvement in the device efficiency. However, several recombination processes also occur at this interface which affects the overall device efficiency. Both injection and recombination dynamics are influenced by the electronic coupling between the dye and TiO_2 and therefore, the binding mode of the dye to the TiO_2 surface. Therefore, the efficiency of the DSSCs, in addition to TiO_2 CBE movement, depends upon the interaction of the dye molecules with the TiO_2 surface.

In spite of the fact that modified TiO_2 surface might lead to a change in the electron injection dynamics owing to different binding mechanism of N719 dye molecules on the modified surface, this aspect has not been discussed in literature and there is no report yet describing the binding mechanism of the ruthenium complexes onto surface modified TiO_2. Nevertheless, the absorption orientation and electronic coupling of N719 on TiO_2 has been studied and discussed by several groups using vibrational spectroscopy, X-ray absorption spectroscopy and computational model studies. Despite the volume of work, the binding mechanism of N719 dye onto TiO_2 surface is not yet fully understood and remains a subject of debate. The various binding mechanisms proposed in literature are summarized in Fig.1 and elaborated as follows. The structure of N719 dye is shown in Fig. 1(a). As shown in Fig.

1 (b), first type of binding, known as ester type linkage, involves interaction of one or two oxygen atom of -COOH group with the Ti atoms of TiO_2 surface, resulting in unidentate or bidentate co-ordination mode. Falaras et al suggested this type of linkage based on 20 cm^{-1} shift in carbonyl group observed in FTIR spectra[9]. The second type of binding involves the interaction of both the oxygen atoms of COOH groups with either one Ti or two Ti atoms resulting in bidentate chelating or bridging, as depicted in Fig. 1 (c) and (d). This mechanism was proposed by Finnie et al, who studied the co-ordination of the dyes and of benzoic acid onto TiO_2 surface[10]. Based on their results they suggested that carboxylate attaches to the TiO_2 surface via bidentate chelating or bridging co-ordination using two carboxylic acid groups per dye molecule. Later, Nazeeruddin at al investigated different ruthenium complexes to determine the specific carboxylic group (COO^- or -COOH) involved in TiO_2 binding[11]. Based on FTIR analysis, they deduced that N719 dye absorbs on the TiO_2 surface in bridging mode via two carboxylic groups trans to the NCS group. Further, support data were provided by Leon et al who carried out UV-vis, FTIR and Raman to investigate the absorption mechanism of N719 sensitizer on TiO_2[12]. From the Raman measurements, the co-ordination of the N719 dye was proposed to occur through bridging or bidentate linkage. They confirmed their results by the ATR-FTIR spectra which provided a direct finger print of the deprotonation state of the carboxylic moieties. A third binding mechanism was also proposed, see Fig. 1e, on the basis of molecular dynamics simulations and electronic structure calculations. Accordingly, the N719 dye binding to the TiO_2 surface occurs through three carboxylic groups, one of which is attached to two Ti atoms in bidentate form while the other two are bound via monodentate mode[13]. In contrast to these findings, a fourth binding mechanism (Fig. 1f), was also proposed where the N719 dye molecules interact with the TiO_2 surface though the NCS group in addition to the bidentate bridging[14]. Recent studies by Lee et al elucidated the role of Ti-OH/$TiOH_2$ groups in the binding mode of the dye[15]. On the basis of detailed vibrational spectroscopic studies of N719 dye absorbed on TiO_2 surface they proposed that the binding of the dye to TiO_2 occurs through two neighboring carboxylic acid/carboxylate groups via a combination of bidentate-bridging and H-bonding involving a donating group from the N719 dye and acceptor from the Ti-OH group (Fig. 1g).

Though, most studies suggest anchoring of N719 dye on the TiO_2 surface via two carboxylate groups, the role of various kind of surface treatments of TiO_2 surface has not been reported so far. In our earlier work, we had reported that the efficiency of the DSSC is improved significantly when a photoanode consisting of N3 dye loaded onto formic acid treated TiO_2 surface or N719 dye loaded onto carboxylic acid treated TiO_2 surface are

utilized[16-17]. The analyses of the device characteristics in both the cases revealed that the efficiency improvement occured due to enhanced dye absorption onto TiO_2 electrode and reduced recombination. This resulted in an increase in both the J_{SC} and V_{OC}, and thereby enhanced efficiency.

In this work, we report a detailed investigation of the binding mechanism of N719 dye onto the oxalic acid treated TiO_2 surface using various characterization techniques i.e. X-ray absorption fine structure (EXAFS) measurements, Fourier transform infrared spectroscopy (FTIR), UV-Vis spectroscopy and X-ray photoelectron spectroscopy (XPS). The results of these studies revealed that the binding of N719 molecules takes place via interaction between Ru atom of the dye and O^- of bidentate bridged oxalate ions at TiO_2 surface. This is in contrast to the binding of N719 onto untreated TiO_2 surface, where -COOH and SCN groups of the dye directly bind to TiO_2 surface. The results of incident photon to current conversion efficiency (IPCE) measurements show that presence of oxalate ions between dye and TiO_2 surface favors efficient electron transfer, and therefore, improves the device efficiency.

2. EXPERIMENTAL

2.1 Fabrication of DSSC:

The photoelectrode was fabricated using the procedure reported earlier[17]. Briefly, TiO_2 compact layer was deposited on the fluorine doped tin oxide (FTO, Solaronix, TCO22-7) by dipping the substrate into $TiCl_4$, followed by an annealing at 450°C for 30 mins. A mesoporous TiO_2 was subsequently deposited from precursor paste (Solaronix, Ti-Nanoxide HT) by doctor blading. The electrodes were sequentially annealed at 75°C for 10 mins, 135°C for 10 mins, 175°C for 20 mins, 425°C for 10 mins and 450°C for 10 mins. The TiO_2 electrode thus prepared were treated with oxalic acid (0.05 M in ethanol solution) for 1 hr, then washed in ethanol thoroughly and finally, dried in N_2 flush. Hereafter untreated TiO_2 and oxalic acid treated TiO_2 will be referred as WO-TiO_2 and OA-TiO_2 electrodes, respectively. For dye sensitization, both WO-TiO_2 and OA-TiO_2 electrodes were dipped in N719 dye solution (0.3mg/ml in ethanol) for 24 hrs, and henceforth these electrodes will be referred as N719_WO-TiO_2 and N719_OA-TiO_2, respectively. The DSSC (area~0.1 cm^2) was assembled by clipping together a photoelctrode and Pt electrode having 20μm spacer. A solution of 0.1 M LiI and 0.05 M I_2 in dry acetonitrile was used as an electrolyte.

2.2 Characterization of the oxalic acid treated electrode:

The current-voltage (J-V) characteristics of the cells were recorded on a Potentiostat/Galvanostat (PGSTAT 30, Autolab Eco Chemie, Netherlands) under the irradiation of 100 mW/cm^2 at AM 1.5 G using solar simulator (Sciencetech, Canada). Prior to the measurements, the intensity of the solar simulator was calibrated using a reference silicon solar cell. In order to estimate dye loading, the UV/Vis spectroscopy was carried out using a double beam UV/Vis spectrophotometer (Jasco, V 530) and all spectra were baseline corrected for quantitative analysis. The extent of dye loading was estimated by desorbing a dye sensitized electrode (area~1 cm^2) from 0.1M aqueous KOH (2ml) solution and then recording the absorbance spectrum. The binding modes of oxalic acid on the TiO_2 surface as well as with dye molecules after treating the TiO_2 surface with oxalic acid, were deduced from FTIR spectroscopy using Bruker spectrometer (model: Vertex 80 V) at a resolution of 4 cm^{-1}. In order to investigate further the anchoring mode of the N719 dye molecules to the oxalic acid treated TiO_2 surface, XPS was carried out using Mg K_α source (RIBER MBE system). The binding energy scale was calibrated to the Au $4f_{7/2}$ line of 83.95 eV. Since, in the 1400-1600 cm^{-1}, the actual binding mode of ruthenium complexes is often hindered due to the overlapping absorptions, we confirmed the results by using EXAFS, which is a useful technique for probing the co-ordination changes occurring around the element of interest. EXAFS experiments were carried out at Deutsches Elektronen Synchrotron (DESY), Hamburg, Germany, at the P06 beamline in transmission mode. The energy calibrations were carried out using the characteristics Ru k-edge at 22127 eV of ruthenium.

3. RESULTS AND DISCUSSION

Fig. 2 shows typical photovoltaic characteristics of the DSSCs fabricated using N719_OA-TiO_2 and N719_WO-TiO_2 photoanodes under illumination of AM 1.5G (intensity = 100 mW/cm^2). As shown in the figure, the photovoltaic parameters of the devices fabricated using N719_OA-TiO_2 are superior to that fabricated using N719_WO-TiO_2 electrodes. The overall efficiency of 4.6% (±0.1) is obtained for the device using N719_OA-TiO_2 photoanodes as compared to 3.2% (±0.16) device efficiency using N719_WO-TiO_2 electrodes. The detailed analyses of various photovoltaic parameters of devices are presented in our earlier paper[17]. It has been demonstrated that OA-treatment of TiO_2 leads to the following beneficial effects: (i) improvement in V_{OC} due to the CBE and quasi Fermi level shift as well as reduced recombination, (ii) increase in the amount of dye loading on e.g. the amount of N719 dye loaded onto OA-TiO_2 was 3.2×10^{-5} mole/cm^2, which is significantly

higher than that onto TiO_2 electrodes (2.3×10^{-5} mole/cm^2). In this paper, we focus on the investigation of the binding mechanism of N719 dye onto oxalic acid treated TiO_2 electrode, using various techniques as discussed below.

3.1 UV-Vis Spectroscopy:

The UV-Vis spectra of dye loaded on WO-TiO_2 and OA-TiO_2 were recorded taking TiO_2 as reference electrode and the results are presented in Fig.3a. As shown in the figure, the N719 dye exhibits peaks at 399 nm and 540 nm corresponding to metal-to-ligand charge transfer (MLCT) transition. It may be noted that the higher energy MLCT has some character for π-π* (ligand centered) transition. Major inferences drawn from this figure are:

(i) The absorbance of the dye loaded onto OA-TiO_2 is higher than that onto WO-TiO_2 electrodes, which corroborates our earlier results that higher N719 dye loading takes place onto OA-TiO_2 electrodes.

(ii) The low energy MLCT band reveals a blue shift from 540 nm to 525 nm for N719 dye loaded onto OA-TiO_2 electrodes. The blue shift may be attributable to an increase in the energy of the LUMO of the ligand, causing π -π* transitions to occur at higher energies. Since the shape of the absorbance curve has not changed, we rule out dye aggregation as the cause of this shift. Therefore, this blue shift might arise due to an interaction between N719 dye and the oxalate ions present on the TiO_2 surface.

(iii) There is a slight red shift in higher energy MLCT band from 399 to 407 nm for N719_OA-TiO_2. This is expected to have resulted from the increased delocalization of π-electron in the system for N719_OA–TiO_2 electrodes. This suggests that the anchoring of the N719 dye to OA-TiO_2 is different from anchoring of the dye on WO-TiO_2 electrode. In order to understand the effect of the type of dye anchoring on device efficiency, we examined the anchoring mechanism of the dyes on the OA-TiO_2 electrodes using various spectroscopic techniques as discussed below.

3.2 Fourier Transform Infrared (FTIR) Spectroscopy:

Before analyzing how the dye is anchored onto OA-TiO_2 electrodes, we first investigated the changes that occurred to TiO_2 surface when subjected to oxalic acid treatment. For the purpose, we recorded the FTIR spectra of OA-TiO_2 as well as that of TiO_2 electrodes and the results are shown in Fig. 3b. The FTIR spectra of oxalic acid absorbed on TiO_2 shows two bands at 1731 and 1697 cm^{-1}, which are due to splitting of two similar

carbonyl (C=O) groups[18]. These bands are assigned to either bidentate chelating or bidentate bridging ring structure with one oxygen of each carboxylic group co-ordinated to the surface sites and two C=O double bonds pointing away from the surface. DFT calculation and ATR FTIR spectroscopic results by Mendive et al propose the existence of both types of binding modes at the TiO_2 surface[19]. The increase in loading of N719 dye OA-TiO_2 electrode as discussed earlier may be attributed to the bridging mode of oxalic acid on TiO_2 surface. Further, we recorded the FTIR spectra for dye loaded onto WO-TiO_2 as well as OA-TiO_2 electrode and normalized the spectra using intensity of the bipyridine (C=C) at 1542 cm^{-1} as an internal standard (Fig. 4 a and b). The peak assignments are summarized in Table1.

The IR spectra of the free dye show the presence of carboxylic acid and carboxylate groups as evident by the $\upsilon_{C=O,}$ υ_{C-O} and $\upsilon_{COO^-,asym}$ and $\upsilon_{COO^-,sym}$ vibrational modes[10]. In case of dye loaded on WO-TiO_2, the asymmetric and symmetric stretching modes of COO^- are observed at 1615 cm^{-1} and 1373 cm^{-1} respectively[10]. On the other hand, these bands are shifted to slightly higher binding energy (~ 6 cm^{-1}) in case of N719 dye loaded onto OA-TiO_2 surface. This suggests that interaction of N719 dye molecules on OA-TiO_2 surface is different from that on WO-TiO_2 surface. In addition to these peaks, two bands at 1698 and 1719 cm^{-1} are also observed in the N719 dye loaded onto OA-TiO_2 electrode, these bands arise due to carbonyl group of oxalic acid as well as that of the dye. The relative intensity of the band at 1719 cm^{-1} with respect to that at 1698 cm^{-1} is decreased implying the involvement of oxalate ions present at the TiO_2 surface in the binding of N719 dye. Further, the occurrence of TBA peaks in case of dye loaded onto WO-TiO_2 and OA-TiO_2 rules out the possibility of anchoring of the dye through covalent bonding of carboxylate groups. It was suggested by Hirose et al that in order to dissociate TBA from the N719 molecule, it must react with the Ti-OH/$TiOH_2$ groups[20-21]. The difference ($\Delta\nu$) between $\upsilon_{COO^-,asym}$ and $\upsilon_{COO^-,sym}$ vibrational modes has been related to the type of co-ordination mode of carboxylate group to metal ions by an empirical rule derived by Deacon and Phillips[22]. In particular, the solid state ($\Delta\nu_{salt}$) and the absorbed state ($\Delta\nu_{ads}$) have been used to determine bond coordination in carboxylate and carboxylic acid groups. Accordingly, the nature of binding mode can be inferred from the following criterion: if $\Delta\nu_{ads} > \Delta\nu_{salt}$, the bonding is unidentate but if $\Delta\nu_{ads} < \Delta\nu_{salt}$ the chelate or bridge mode occurs. Under the condition, when $\Delta\nu_{ads} <<< \Delta\nu_{salt}$, the chelating is the binding mode. The $\Delta\nu$ value for free dye and the dye absorbed onto WO-TiO_2/OA-TiO_2 is 252 and 242 cm^{-1}, respectively, suggesting bidentate chelating or bridging bonding. It may be noted here that this mode could arise because of bidentate chelating or bridging bonding of COO^- group of oxalate ions present at the TiO_2 surface in case of dye loaded on OA-TiO_2 electrode.

In order to further clarify the binding mechanism, we have focused in region 1000-2200 cm^{-1} (Fig. 4a), where peaks corresponding to C=O, COO- and NCS appear. The major observations from this region are:

(i) The peak corresponding to C=O is present in case of free dye as well as N719 dye on WO- and OA-TiO_2 electrodes, suggesting that some of the absorbed dye is not bound to the TiO_2 surface via bidentate chelating or bridging bonding mode and some additional binding modes of N719 dye to the WO- and OA-TiO_2 electrodes may be present.

(ii) The peak corresponding to $\upsilon_{N=C}$ of NCS group is shifted towards lower wavenumber (from 2102 to 2095 cm^{-1}) when the dye is absorbed onto WO-TiO_2 surface. Though such observations were also made by previous studies, the role of NCS in binding of the N719 dye to TiO_2 electrode was not elaborated much. It was suggested by Johansson et al[14] as well as Lee et al[15] that N719 dye may also bind to the TiO_2 surface through NCS group. The striking features of the dye absorbed onto OA-TiO_2 electrode are (a) a large shift of ~10 cm^{-1} towards lower wavenumbers and (b) significant reduction in intensity of this peak.

These observations suggest that NCS group plays a significant role in the anchoring of N719 dye to the OA-TiO_2 surface. This is also confirmed by the disappearance of the 843 cm^{-1} peak corresponding to C=S groups in case of N719 dye sensitized OA-TiO_2 electrode (Fig. 4b). The peak at 832 cm^{-1} is assigned to C=S of NCS group of the N719 dye absorbed onto WO-TiO_2 electrode. However, this peak is missing and instead an intense peak is observed at 864 cm^{-1} in case of N719 dye sensitized on OA-TiO_2 electrode. This peak cannot be assigned to the C=S stretching mode. The reason is that the intensity of peak corresponding to NCS is very less in N719_OA-TiO_2 electrode as compared to that of N719_WO-TiO_2 electrode and therefore, we should have observed very weak peak, if any, corresponding to C=S bond. This peak is assigned to Ru-O, which might have resulted owing to the interaction of the N719 dye with oxalate ions present at the OA-TiO_2 surface[23].

Further, the relative amount of bound N719 dye molecules on the TiO_2 surface has been estimated by the relative intensity of the peak at free carboxylic acid (C=O, 1723 cm^{-1}) and carboxylate groups (COO^-, 1373 cm^{-1})[24-25]. Since for OA-TiO_2 electrode, the carbonyl group peak at 1719 cm^{-1} has contributions from the dye as well as oxalic acid, it is difficult to determine quantitatively the amount of N719 dye on the OA-TiO_2 surface.

Nevertheless, the decrease in the intensity of this peak may be related to the increased amount of dye loading on the OA-TiO_2 surface as compared with WO-TiO_2 one. This corroborates with our results on amount of higher N719 dye loading on OA-TiO_2 surface as compared with WO-TiO_2 one. The presence of more N719 dye molecules on the OA-TiO_2 electrode then resulted in enhanced light harvesting and additional photoinduced electrons in DSSC as compared with WO-TiO_2 electrodes[26].

3.3 X-ray Photoelectron Spectroscopy:

In order to further confirm our findings of FTIR spectra, we have recorded XPS spectra of N719 dye loaded on WO-TiO_2 and OA-TiO_2. XPS is highly surface sensitive technique to distinguish between different chemical states of the same atom and the obtained findings are discussed below:

Ti 2p: As shown in Fig.5, the splitting due to spin-orbit coupling is observed in case of dye sensitized on WO-TiO_2 and OA-TiO_2 electrode. These Ti 2p peaks at 459.3eV and 465.1eV are attributable to Ti^{4+} $2p_{3/2}$ and Ti^{4+} $2p_{1/2}$ states, respectively. This suggests that the surface of TiO_2 electrodes comprise of titanium(IV) dioxide only and suboxides i.e. TiO, Ti_2O_3 etc. are not present[15]. In case of dye sensitized on OA-TiO_2, these Ti 2p peaks are shifted to slightly higher binding energies as compared to that of WO-TiO_2. The shift to higher binding energies could be due to change in the surface dipole and/or change in the Fermi level position in the band gap as a result of oxalic acid treatment of TiO_2 surface. Such changes were also reflected in the UV-Vis spectrum, where a blue shift of 15 nm is observed for dye sensitized OA-TiO_2 electrodes. In addition to the shift in B.E., a decrease in intensity of Ti2p peaks is also observed indicating absorption of oxalate ions on TiO_2 surface.

C1s: The C 1s spectra of dye sensitized WO-TiO_2 and OA-TiO_2 are shown in Fig. 6 (a, b). The spectra reveals four peaks upon deconvolution having full width-half maximum (FWHM) of 1.48 and 1.46 eV for N719_WO-TiO_2 and N719_OA-TiO_2, respectively. It is to be noted here that the Ru $3d_{3/2}$ peak is hidden under the major C 1s peak (285.9eV)[27]. The XPS studies of pyridine and pyridine-carboxylic acid adsorbed on TiO_2 surface showed that C 1s peaks due to pyridine ring and carboxylic group occur at 284eV and 289eV, respectively[28]. However, in case of dye sensitized TiO_2, the main C 1s peak contains contributions from TBA and NCS groups as well. Therefore, the main C 1s peak at 285.9eV is contributed by C=C, C-C, C-O, C=N, TBA and Ru $3d_{3/2}$. The smaller peaks at 288.3eV and

289.6eV are attributed to O-C=O/C=O from COOH/COO^- groups and adsorbed CO_2, respectively[29]. The contributions from the adsorbed organic contaminants in the sample is associated with the peak at 286.9eV[30]. C1s XPS spectrum for dye sensitized OA-TiO_2 electrode upon deconvolution shows similar peaks as that of WO-TiO_2 electrode loaded with N719 dye. However, a small shift in peak positions to higher binding energy is observed indicating that the chemical environment of the C is changed when TiO_2 is treated with oxalic acid.

O 1s: The O 1s spectra can provide information about the bonding interaction and surface geometrical structure of the anchoring group. The O 1s XPS spectra of dye sensitized WO-TiO_2 and OA-TiO_2 both exhibit asymmetrical broadening towards the higher binding energy side, as shown in Fig. 6 (c, d). The deconvolution of the dye sensitized TiO_2 shows four well resolved peaks, FWHM for all the fitted peaks of N719_WO-TiO_2 and N719_OA-TiO_2 are 1.67 and 1.65 eV, respectively. The peaks at 530.5eV, 531.9eV is attributable to O^- and Ti-OH from TiO_2 surface, respectively. The peak at 531.9 eV has also some contribution from C=O group of the dye. The peak at 533.2 eV is assigned to COOH groups of the dye as well as Ti-OH_2. In addition, the peak at 534.5eV is attributable to the adsorbed organic contaminants. The observed deconvoluted peaks are in accordance with those reported in literature[15]. When the N719 dye is loaded onto WO-TiO_2 electrode, the peak corresponding COOH and C=O groups of the dye are shifted to lower binding energy side. This suggests that the chemical environment around O is different from dye loaded WO-TiO_2 electrode. The main feature of O 1s XPS spectrum of N719 sensitized on OA-TiO_2 is the appearance of new well resolved peak at 529.5eV and disappearance of peak corresponding to the O^- at WO-TiO_2 surface. The new peak at 529.5eV is assigned to Ru-O bond[31-32]. The origin of this new peak may be due to the substitution of NCS group of the dye by O^- of the oxalic acid. In addition, the disappearance of O^- peak could be due to large electron scattering arising due to presence of oxalate ions and dye layer on WO-TiO_2 surface.

Ru $3d_{5/2}$: The splitting due to spin-orbit coupling is observed corresponding to the Ru of the dye, i.e.Ru $3d_{3/2}$ and Ru $3d_{5/2}$. The Ru $3d_{3/2}$ peak overlaps with C 1s peak, and therefore, it is difficult to extract information by deconvolution of this peak. However, Ru $3d_{5/2}$ peak reveals a shift of 4.2eV from Ru $3d_{3/2}$ peak[27]. Therefore, Ru $3d_{5/2}$ peak can be utilized to extract further the information about the chemical state of Ru. Fig. 6(e, f) shows the XPS spectrum of Ru$3d_{5/2}$ for N719 dye sensitized onto TiO_2 and OA-TiO_2. In case of Ru, FWHM for all the

fitted peaks of N719_WO-TiO_2 and N719_OA-TiO_2 are 1.63 and 1.64eV, respectively. As shown in fig. 6e, the peak at 281.3eV is attributed to Ru $3d_{5/2}$ arising due to the adsorbed N719 dye molecules on the WO-TiO_2 surface[15]. In case of N719 loaded onto OA-TiO_2, the Ru $3d_{5/2}$ is deconvoluted in two peaks: peak at 281.9eV is attributable to the dye molecules absorbed on TiO_2 surface as in case of N719_WO-TiO_2 surface, while a well resolved peak at 280.1eV is assigned to the Ru-O bond. This Ru-O bond occurs due to chemical bond involved between dye molecules and oxalate ions present at OA-TiO_2 surface. This is in line with our earlier observation in FTIR data where, signature of Ru-O bond is observed in dye loaded onto OA-TiO_2 electrode.

S2p: The S 2p spectra of N719 dye loaded onto WO-TiO_2 shows contributions from the sulfur of NCS group owing to spin-orbit coupling. This is similar to the reports by other researchers where two peaks are observed and assigned to the contributions arising from the interaction between the NCS ligand and the dye. More strikingly, these peaks are not observed in case of N719 dye sensitized onto OA-TiO_2, as shown in Fig. 7. This confirms our earlier assumption based on FTIR data and O1s XPS data that NCS group of the N719 dye is substituted by the O^- group of oxalate ions present at the OA-TiO_2 surface.

3.4 Extended X-ray Absorption Fine Structure:

Since NCS ligand is the weakest one in the dye molecule, it is likely to be replaced more easily vis a vis the other carboxylate or carboxylic acid group ligand upon absorption onto TiO_2 surface as suggested by our FTIR and XPS data. In order to confirm this, we have focused on Ru atom and its surroundings and recorded EXAFS spectra in spectral region extending from 100 eV below and 1000 eV above a core level excitation k-edge of ruthenium. After the atomic background absorption subtraction, the EXAFS (χ) was extracted from the measured data. For a quantitative comparison of the local structural properties, the data was Fourier transformed to R- space. A set of EXAFS data analysis program available within IFEFFIT software package has been used for fitting of experimental data using the following equation:

$$\chi = \sum_j \frac{N_j f_j(k) \exp\left[-2k^2\sigma_j^2\right] \exp\left[\frac{-2R_j}{\lambda}\right]}{kR_j^2} \sin\left[2kR_j + \delta_j(k)\right]$$

Where $f(k)$, $\delta(k)$, λ, N_j being the amplitude function, phase shift, mean free path of electron and number of atoms in jth shell, respectively. While fitting the data, bond distance (R), co-ordination number (N) and disorder (Debye-Waller) factor (σ^2) were used as fitting parameters. As shown in fig. 1 (a), N719 dye has a complex structure having two nitrogen atoms bonded to NCS group and four nitrogen bonded to the bypyridine ligand. Owing to the complex structure, we have fitted only first two peaks of EXAFS spectra. In case of N719_WO-TiO_2, these peaks correspond to first two co-ordination shells having 2 and 4 nitrogen atoms, respectively as shown in Fig. 8(a). The parameters derived from fitting results are summarized in Table 2. As shown in the table, the bond lengths for Ru and nitrogen are 2.052Å and 2.108Å, respectively for nitrogen bonded at NCS group and bypyridine, respectively. These bond lengths values are similar to the ones reported in literature for free N719 dye[33]. A slight deviation of the bond lengths could arise because of the chemical bonding of N719 to the WO-TiO_2 surface.

However, for N719_OA-TiO_2, reasonable fitting could not be established under these assumption, i.e. when we attempted to fit data considering only first two co-ordination shells of nitrogen atoms. When Ru-O bonding was taken into account as revealed from our XPS and FTIR data, best fitting was obtained as shown in Fig. 8(b). Therefore, in this case, three co-ordination shells were considered during fitting, first co-ordination shell having one oxygen atom, second having one nitrogen atom and third having 4 nitrogen atoms. The Ru-N bond length deduced from the fitting curves are 2.057 Å and 2.125 Å corresponding to nitrogen at NCS group and bypyridine, respectively. These values are almost same as that in case of N719_WO-TiO_2. In addition the Ru-O bond length, as estimated from the fitting, is 1.657 Å which is in agreement to the values reported in literature[34].

3.5 Proposed binding scheme and implication of dye binding on photovoltaic properties:

On the basis of all spectroscopic and EXAFS data, we propose the binding of N719 dye on WO-TiO_2 and OA-TiO_2 surfaces. In the proposed model, N719 dye molecules adsorbs on WO-TiO_2 surface via the COOH groups as well as through some interaction via NCS group, as shown in Fig. 1 (f). However, the anchoring of the N719 dye via carboxylate/carboxylic acid groups is ruled out at the OA-TiO_2 surface. Since NCS is weakest ligand in the N719 dye, the possibility of binding of the N719 dye to the OA-TiO_2 surface through this group is more than via the carboxylate/carboxylic acid groups. This was

complemented by our FTIR data, where a peak corresponding to NCS diminishes significantly. The same is also confirmed by EXAFS data, where a better fitting is observed corresponding to Ru-O bond and not Ru-NCS bond. Therefore, based on these results it is suggested that the N719 dye binds to the OA-TiO_2 surface through interaction between Ru atom of the dye and O^- present at OA-TiO_2 surface due to oxalate ions, as shown schematically in Fig 9.

The role of oxalic acid treatment of TiO_2 surface can thus be summarized as follows:

(i) The binding of the N719 via carboxylate ions present at the OA-TiO_2 surface may allow more effective transfer of electrons owing to increased conjugation as compared to untreated TiO_2 surface[35].

(ii) Being a strong acid (pKa = 1.23), the oxalic acid chelates to Ti atoms on TiO_2 surface via bridging binding strongly and allow more dye loading onto OA-TiO_2 electrode as discussed earlier.

(iii) In addition to providing assistance for more dye loading, the oxalic acid occupied sites also act as a passivation layer. This was confirmed in our earlier observations on impedance spectroscopy measurements, where an increased recombination life time is observed for OA-TiO_2 based DSSC[36].

4. CONCLUSION

In summary, we have studied the binding behavior of the N719 dye through detailed spectroscopic investigation, namely, FTIR, UV-Vis, and XPS spectroscopy, and EXAFS measurements. The UV-Vis spectra implies a strong interaction between the dye and the oxalic acid, which then assist more dye loading onto OA-TiO_2 surface. The FTIR and XPS spectroscopy revealed that binding of N719 dye onto OA-TiO_2 surface is different from that onto WO-TiO_2 electrode: The N719 dye binds to the OA-TiO_2 surface through interaction between Ru atom of the dye and O^- present at OA-TiO_2 surface due to oxalate ions, on the other hand the binding of the dye to untreated TiO_2 surface occurs through carboxylic acid group. The results were confirmed by EXAFS measurements, which also show reasonable fitting for Ru-O bond in case of N719_OA-TiO_2 electrodes. The different binding mechanism of the N719 dye on oxalic acid treated TiO_2 electrode resulted in improved photovoltaic characteristics of DSSCs based on N719 dye sensitized OA-TiO_2 electrodes.

5. ACKNOWLEDGEMENTS

This work is supported by "DAE-SRC Outstanding Research Investigator Award" (2008/21/05-BRNS) granted to D.K.Aswal. We are grateful to SINP-DST for providing financial assistance to carry out experiments at DESY, Hamburg, Germany. We are also thankful to Dr. G.Falkenberg, Hamburg, DESY for his kind help during the EXAFS measurements.

6. REFERENCES

1. 1.Lee, C.-H.; Hsiao, P.-T.; Lu, M.-D.; Wu, J.-M., Light Harvesting Enhancement for Ti-based Dye-Sensitized Solar Cells by Introducing a Grooved Texture Underlayer. *RSC Advances* **2013,** *3*, 2216-2218.
2. Liu, G.; Li, X.; Wang, H.; Rong, Y.; Ku, Z.; Xu, M.; Liu, L.; Hu, M.; Yang, Y.; Han, H., An Efficient Thiolate/disulfide Redox Couple based Dye-Sensitized Solar Cell with a Graphene Modified Mesoscopic Carbon Counter Electrode. *Carbon* **2013,** *53*, 11-18.
3. Manseki, K.; Yu, Y.; Yanagida, S., A Phenyl-Capped Aniline Tetramer for Z907/tert-butylpyridine-based Dye-Sensitized Solar Cells and Molecular Modelling of the Device. *Chem. Commun.* **2013,** *49*, 1416-1418.
4. Yang, X.; Yanagida, M.; Han, L., Reliable Evaluation of Dye-Sensitized Solar Cells. *Energy & Environmental Science* **2013,** *6*, 54-66.
5. Wang, Z.-S.; Yamaguchi, T.; Sugihara, H.; Arakawa, H., Significant Efficiency Improvement of the Black Dye-Sensitized Solar Cell through Protonation of TiO_2 Films. *Langmuir* **2005,** *21*, 4272-4276.
6. Park, K.-H.; Jin, E. M.; Gu, H. B.; Shim, S. E.; Hong, C. K., Effects of HNO_3 Treatment of TiO_2 nanoparticles on the Photovoltaic Properties of Dye-Sensitized Solar Sells. *Mater. Lett.* **2009,** *63*, 2208-2211.
7. Guai, G. H.; Song, Q. L.; Lu, Z. S.; Ng, C. M.; Li, C. M., Tailor and Functionalize TiO_2 Compact Layer by Acid Treatment for High Performance Dye-Sensitized Solar Sells and its Enhancement Mechanism. *Renewable Energy* **2013,** *51*, 29-35.
8. Hao, S.; Wu, J.; Fan, L.; Huang, Y.; Lin, J.; Wei, Y., The influence of Acid Treatment of TiO_2 Porous Film Electrode on Photoelectric Performance of Dye-Sensitized Solar Sells. *Solar Energy* **2004,***76* (6), 745-750.
9. Falaras, P., Synergetic Effect of Carboxylic Acid Functional Groups and Fractal Surface Characteristics for Efficient Dye Sensitization of Titanium Oxide. *Sol. Energy Mater. Sol. Cells* **1998,***53* (1–2), 163-175.
10. Finnie, K. S.; Bartlett, J. R.; Woolfrey, J. L., Vibrational Spectroscopic Study of the Coordination of (2,2-bipyridyl-4,4-dicarboxylic acid)ruthenium(II) Complexes to the Surface of Nanocrystalline Titania. *Langmuir* **1998,** *14*, 2741-2749.
11. Nazeeruddin, M. K.; Humphry-Baker, R.; Liska, P.; Grätzel, M., Investigation of Sensitizer Adsorption and the Influence of Protons on Current and Voltage of a Dye-Sensitized Nanocrystalline TiO_2 Solar Cell. *J. Phys. Chem. B* **2003,** *107*, 8981-8987.
12. León, C.P.; Kador, L.; Peng, B.; Thelakkat, M., Characterization of the Adsorption of Ru-bpy Dyes on Mesoporous TiO_2 Films with UV−Vis, Raman, and FTIR Spectroscopies. *J. Phys. Chem. B* **2006,** *110*, 8723-8730.
13. De Angelis, F.; Fantacci, S.; Selloni, A., Nazeeruddin, M. K.; Grätzel, M., First-Principles Modelling of the Adsorption Geometry and Electronic structure of Ru(II) Dyes

on Extended TiO2 Substrates for Dye-Sensitized Solar Cell Applications. *J. Phys. Chem. C* **2010,** *114*, 6054-6061.
14. Johansson, E. M. J.; Hedlund, M.; Siegbahn, H.; Rensmo, H., Electronic and Molecular Surface Structure of Ru(tcterpy)$(NCS)_3$ and Ru$(dcbpy)_2(NCS)_2$ Adsorbed from Solution onto Nanostructured TiO_2: A Photoelectron Spectroscopy Study. *J. Phys. Chem. B***2005,** *109*, 22256-22263.
15. Lee, K. E.; Gomez, M. A.; Regier, T.; Hu, Y.; Demopoulos, G. P., Further Understanding of the Electronic Interactions between N719 Sensitizer and Anatase TiO_2 Films: A Combined X-ray Absorption and X-ray Photoelectron Spectroscopic Study. *J. Phys. Chem. C* **2011,** *115*, 5692-5707.
16. Saxena, V.; Veerender, P.; Chauhan, A. K.; Jha, P.; Aswal, D. K.; Gupta, S. K., Efficiency Enhancement in Dye Sensitized Solar Sells through Co-Sensitization of TiO_2 Nanocrystalline Electrodes. *Appl. Phys. Lett.* **2012,** *100*, 133303.
17. Saxena, V.; Veerender, P.; Gusain, A.; Jha, P.; Singh, J.; Koiry, S.P.; Varde, P.V.; Chauhan, A.K.; Aswal, D.K.; ,Gupta, S.K.; Co-Sensitization of N719 and RhCL Dyes on Carboxylic Acid Treated TiO_2 for Enhancement of Light Harvesting and Reduced Recombination. *Org. Electron.* **(in press)**.
18. Hug, S. J.; Bahnemann, D., Infrared Spectra of Oxalate, Malonate and Succinate Adsorbed on the Aqueous Surface of Rutile, Anatase and Lepidocrocite Measured with in situ ATR-FTIR. *J. Electron. Spectrosc. Relat. Phenom.* **2006,***150* (2–3), 208-219.
19. Mendive, C. B.; Bredow, T.; Blesa, M. A.; Bahnemann, D. W., ATR-FTIR Measurements and Quantum Chemical Calculations Concerning the Adsorption and Photoreaction of Oxalic Acid on TiO_2. *PCCP* **2006,** *8* , 3232-3247.
20. Hirose, F.; Kuribayashi, K.; Suzuki, T.; Narita, Y.; Kimura, Y.; Niwano, M., UV Treatment Effect on TiO_2 Electrodes in Dye-Sensitized Solar Cells with N719 Sensitizer Investigated by Infrared Absorption Spectroscopy. *Electrochem. Solid-State Lett.* **2008,** *11*, A109-A111.
21. Kuribayashi, K.; Iwata, H.; Hirose, F., N719 Dye Adsorption on Anatase TiO_2 Surfaces Investigated by Infrared Absorption Spectroscopy. *ECS Transactions* **2007,** *6*, 15-19.
22. Deacon, G. B.; Phillips, R. J., Relationships between the Carbon-Oxygen Stretching Frequencies of Carboxylato Complexes and the Type of Carboxylate Coordination. *Coord. Chem. Rev.* **1980,** *33*, 227-250.
23. León, C. P., *Vibrational Spectroscopy of Photosensitizer Dyes for Organic Solar Cells*. Cuvillier: 2006.
24. Lim, J.; Kwon, Y. S.; Park, T., Effect of Coadsorbent Properties on the Photovoltaic Performance of Dye-Sensitized Solar Sells. *Chem. Commun.* **2011,** *47*, 4147-4149.
25. Schiffmann, F.; VandeVondele, J.; Hutter, J. r.; Wirz, R.; Urakawa, A.; Baiker, A., Protonation-Dependent Binding of Ruthenium Bipyridyl Complexes to the Anatase (101) Surface. *J. Phys. Chem. C* **2010,** *114*, 8398-8404.
26. Kilså, K.; Mayo, E. I.; Brunschwig, B. S.; Gray, H. B.; Lewis, N. S.; Winkler, J. R., Anchoring Group and Auxiliary Ligand Effects on the Binding of Ruthenium Complexes to Nanocrystalline TiO_2 Photoelectrodes. *J. Phys. Chem. B* **2004,** *108*, 15640-15651.
27. Cai, T.; Song, Z.; Chang, Z.; Liu, G.; Rodriguez, J. A.; Hrbek, J., Ru Nanoclusters Prepared by $Ru_3(CO)_{12}$ Deposition on Au(111). *Surf. Sci.* **2003,** *538*, 76-88.
28. Schnadt, J.; O'Shea, J. N.; Patthey, L.; Schiessling, J.; Krempaský, J.; Shi, M.; Mårtensson, N.; Brühwiler, P. A., Structural Study of Adsorption of Isonicotinic Acid and Related Molecules on Rutile TiO_2 (110) II: XPS. *Surf. Sci.* **2003,** *544*, 74-86.
29. Guo, Q.; Cocks, I.; Williams, E. M., The Adsorption of Benzoic Acid on a TiO_2(110) Surface Studied using STM, ESDIAD and LEED. *Surf. Sci.* **1997,** *393*, 1-11.

30. Cueto, L.; Hirata, G.; Sánchez, E., Thin-film TiO_2 Electrode Surface Characterization upon CO_2 Reduction Processes. *J. Sol-Gel Sci. Technol.* **2006,** *37*, 105-109.
31. Kim, K. S.; Winograd, N., X-Ray Photoelectron Spectroscopic Studies of Ruthenium-Oxygen Surfaces. *J. Catal.* **1974,** *35*, 66-72.
32. Wier, L. M.; Murray, R. W., Chemically Modified Electrodes: VIII . The Interaction of Aqueous with Native and Silanized Electrodes. *J. Electrochem. Soc.* **1979,** *126*, 617-623.
33. Fantacci, S.; De Angelis, F.; Selloni, A., Absorption Spectrum and Solvatochromism of the [Ru(4,4‘-COOH-2,2‘-bpy)$_2$(NCS)$_2$] Molecular Dye by Time Dependent Density Functional Theory. *J. Am. Chem. Soc.* **2003,** *125*, 4381-4387.
34. Kim, Y. D.; Schwegmann, S.; Seitsonen, A. P.; Over, H., Epitaxial Growth of RuO_2(100) on Ru(10$\bar{1}$0): Surface Structure and Other Properties. *J. Phys. Chem. B***2001,** *105*, 2205-2211.
35. Hara, K.; Sayama, K.; Ohga, Y.; Shinpo, A.; Suga, S.; Arakawa, H., A Coumarin-Derivative Dye Sensitized Nanocrystalline TiO_2 Solar Cell having a High Solar-Energy Conversion Efficiency up to 5.6%. *Chem. Commun.* **2001,** 6, 569-570.
36. Bisquert, J.; Fabregat-Santiago, F.; Mora-Seró, I. n.; Garcia-Belmonte, G.; Giménez, S., Electron Lifetime in Dye-Sensitized Solar Cells: Theory and Interpretation of Measurements. *J. Phys. Chem. C* **2009,** *113*, 17278-17290.

Caption of Figures and Tables:

Figure 1. (a) N719 dye structure and Schematic presentation of binding of N719 dye on TiO_2 surface (b) ester linkage (c) bidentate chelating (d) bidentate bridging (e) Mixed bidentate and monodentate mode (f) NCS group interacts with TiO_2 surface and (g) bidentate chelating and hydrogen bonding.

Figure 2. J-V measurements of the DSSCs based on untreated and carboxylic acid treated TiO_2 electrode sensitized with N719 dye, under AM1.5G intensity 100 mW/cm^2.

Figure 3. (a) UV-Vis spectra of N719 dye loaded TiO_2 and OA-TiO_2 surfaces and (b) FTIR spectra of WO-TiO_2 and OA-TiO_2 surfaces.

Figure 4. FTIR spectra of free N719 dye as well as N719 dye loaded onto WO-TiO_2 and OA-TiO_2 surfaces in (a) 1000-2200 cm^{-1} and (b) 500-800 cm^{-1} frequency range.

Figure 5. XPS spectra of Ti 2p states for N719 dye sensitized TiO_2 and OA- TiO_2 electrode.

Figure 6. XPS spectra of (a, b) O 1s states (c, d) C 1s (e,f) Ru $3d_{5/2}$ for N719 dye sensitized WO-TiO_2 and OA- TiO_2 electrode.

Figure 7. XPS spectra of (a) S and (b) N for N719 dye sensitized TiO_2 and OA- TiO_2 electrode.

Figure 8. The Fourier transforms of the EXAFS function $\kappa^3\chi(\kappa)$ for untreated and carboxylic acid treated dye sensitized TiO_2 samples.

Figure 9. Schematic presentation of binding of N719 dye on oxalic acid treated TiO_2 surface.

Table 1. Peak assignments of the FTIR spectra of the N719 dye sensitized WO-TiO_2 and OA-TiO_2 electrode.

Table 2. Local structural parameters of the N719 dye sensitized WO-TiO_2 and OA-TiO_2 electrode as derived from fitted EXAFS spectra.

Table 1.

Mode of Vibration	**υ(cm^{-1}) N719 dye**	**υ(cm^{-1}) N719_WO-TiO_2**	**υ(cm^{-1}) N719_OA-TiO_2**
Bulk TiO_2	-	554	565
C=S	836	832	Absent
Ru-O	Absent	Absent	864
C-O	1256	1261	1261
Sym (COO^-)	1372	1373	1379
Bpy	1400	1403	1401
TBA	1464	1468	1471
C=C	1540	1541	1545
Asym (COO^-)	1624	1615	1621
C=O (oxalic acid)	Absent	Absent	1698
C=O (dye)	1710	1723	1719
NCS	2102	2095	2085

Table 2

Photoelectrode (coordination shell)	**Parameter**	**N719_WO-TiO_2**	**N719_OA-TiO_2**
Ru-N(1)	N(atoms)	2	1
	R(Å)	2.052±0.03	2.057±0.04
	$\sigma^2(Å^2)$	0.005	0.005
Ru-N(2)	N(atoms)	4	4
	R(Å)	2.108±0.02	2.125±0.05
	$\sigma^2(Å^2)$	0.003	0.006
Ru-O(1)	N(atoms)	-	1
	R(Å)	-	1.657±0.06
	$\sigma^2(Å^2)$	-	0.003

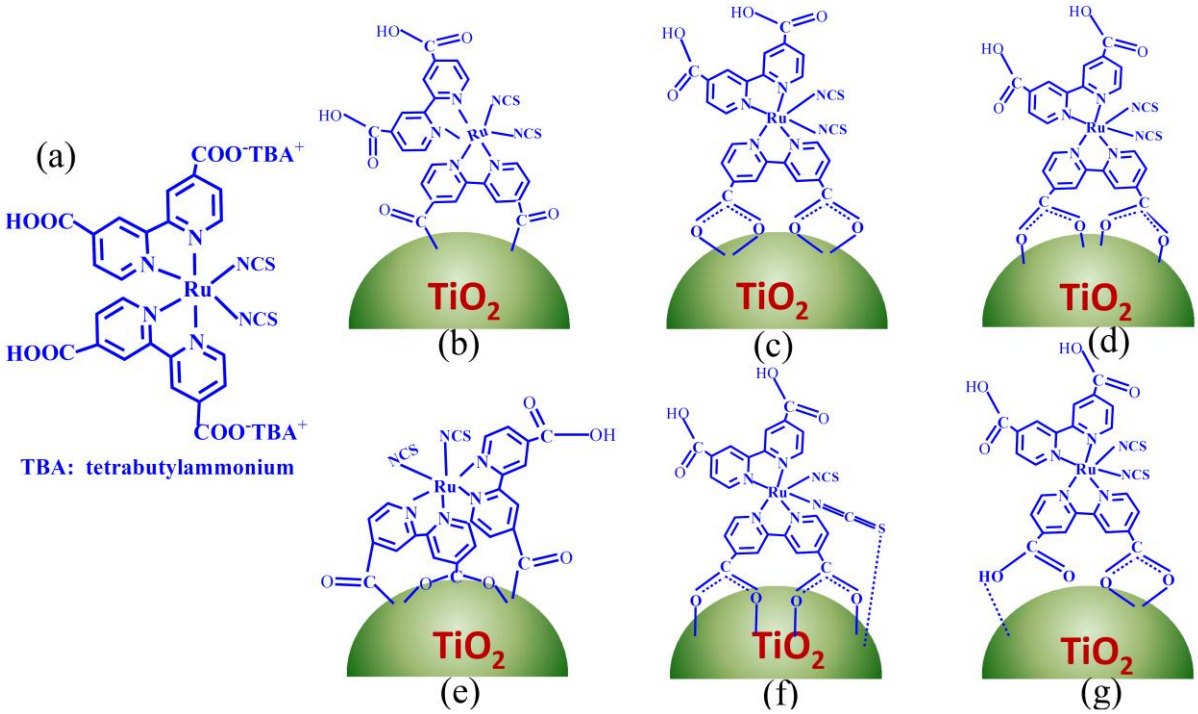
(a)
COO⁻TBA⁺
HOOC
NCS
Ru
NCS
HOOC
COO⁻TBA⁺
TBA: tetrabutylammonium
TiO2
(b)
TiO2
(c)
TiO2
(d)
TiO2
(e)
TiO2
(f)
TiO2
(g)

Fig.1

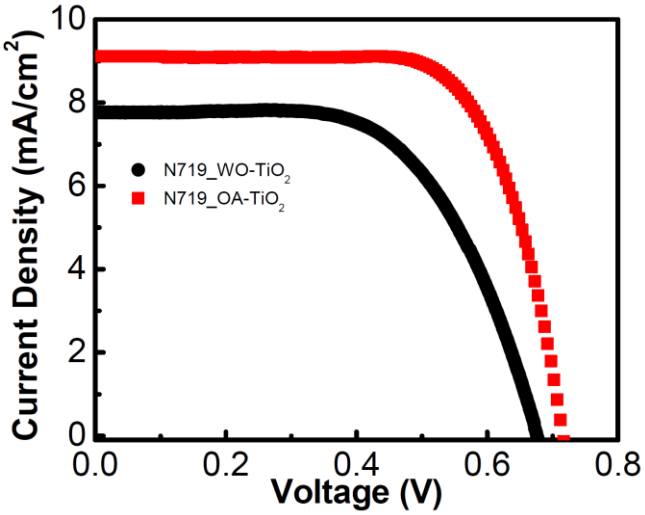
Current Density (mA/cm²)
Voltage (V)
N719_WO-TiO2
N719_OA-TiO2
0
2
4
6
8
10
0.0
0.2
0.4
0.6
0.8

Fig.2

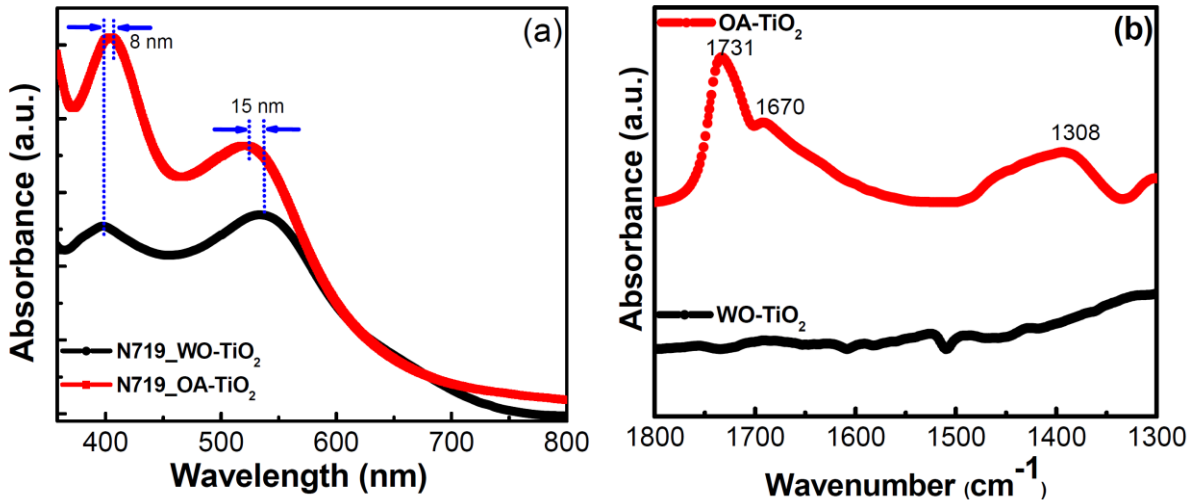
(a)
8 nm
15 nm
Absorbance (a.u.)
N719_WO-TiO2
N719_OA-TiO2
400
500
600
700
800
Wavelength (nm)
(b)
OA-TiO2
1731
1670
1308
WO-TiO2
Absorbance (a.u.)
1800
1700
1600
1500
1400
1300
Wavenumber (cm-1)

Fig.3

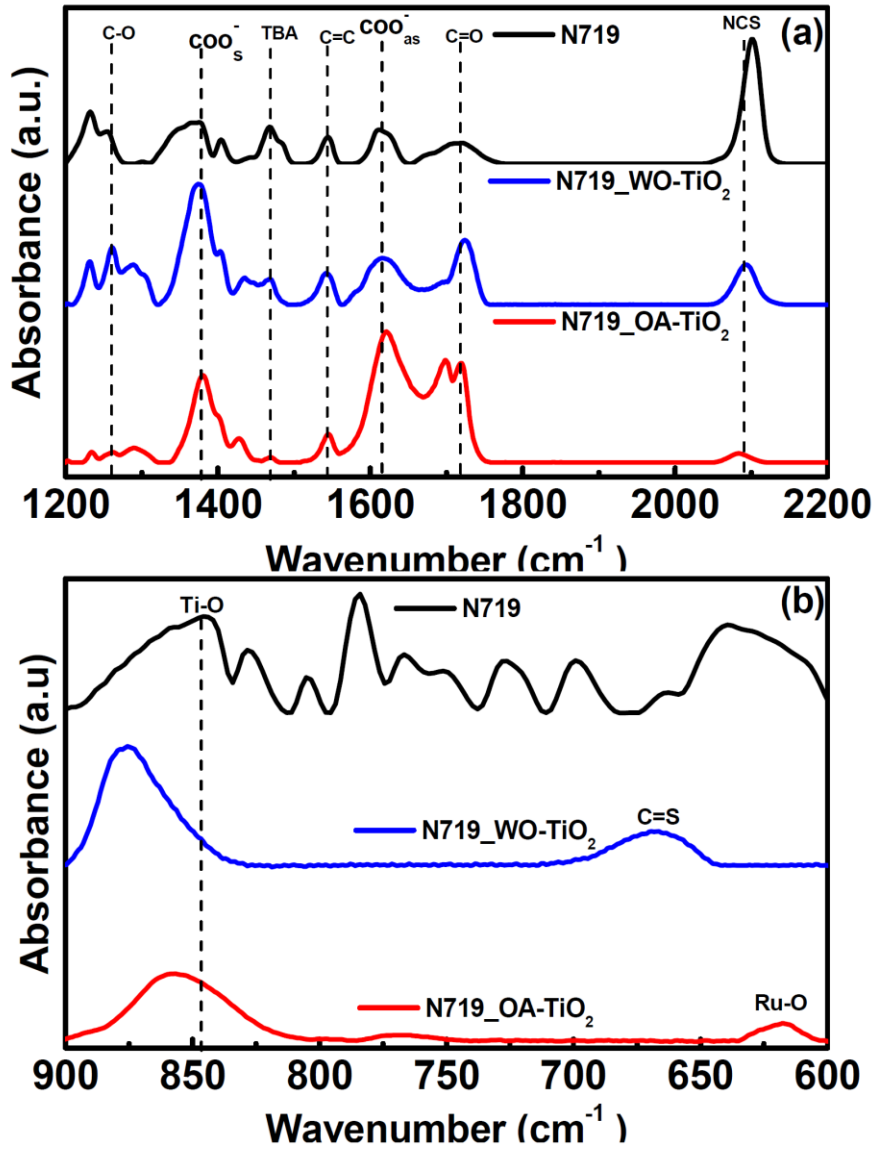
C-O
COO-s
TBA
C=C
COO-as
C=O
N719
NCS
(a)
N719_WO-TiO2
N719_OA-TiO2
Absorbance (a.u.)
1200
1400
1600
1800
2000
2200
Wavenumber (cm-1)
Ti-O
N719
(b)
N719_WO-TiO2
C=S
N719_OA-TiO2
Ru-O
Absorbance (a.u)
900
850
800
750
700
650
600
Wavenumber (cm-1)

Fig.4

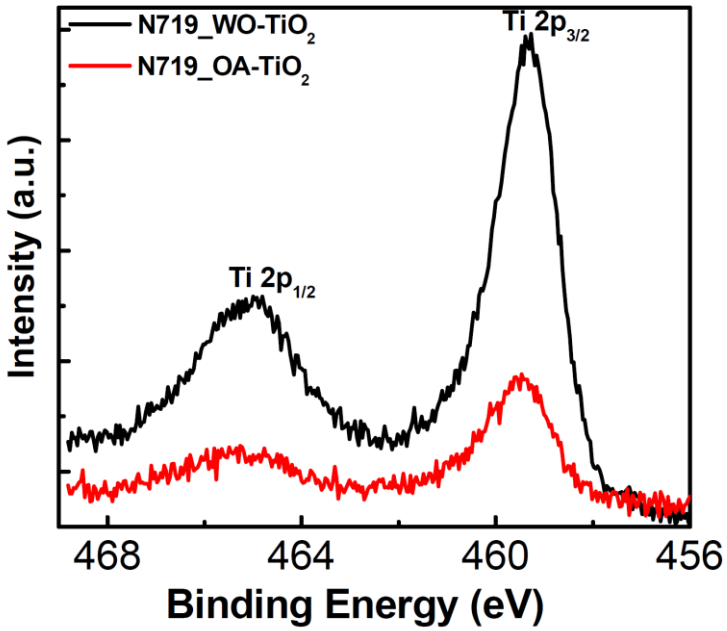
N719_WO-TiO2
N719_OA-TiO2
Ti 2p3/2
Ti 2p1/2
Intensity (a.u.)
468
464
460
456
Binding Energy (eV)

Fig.5

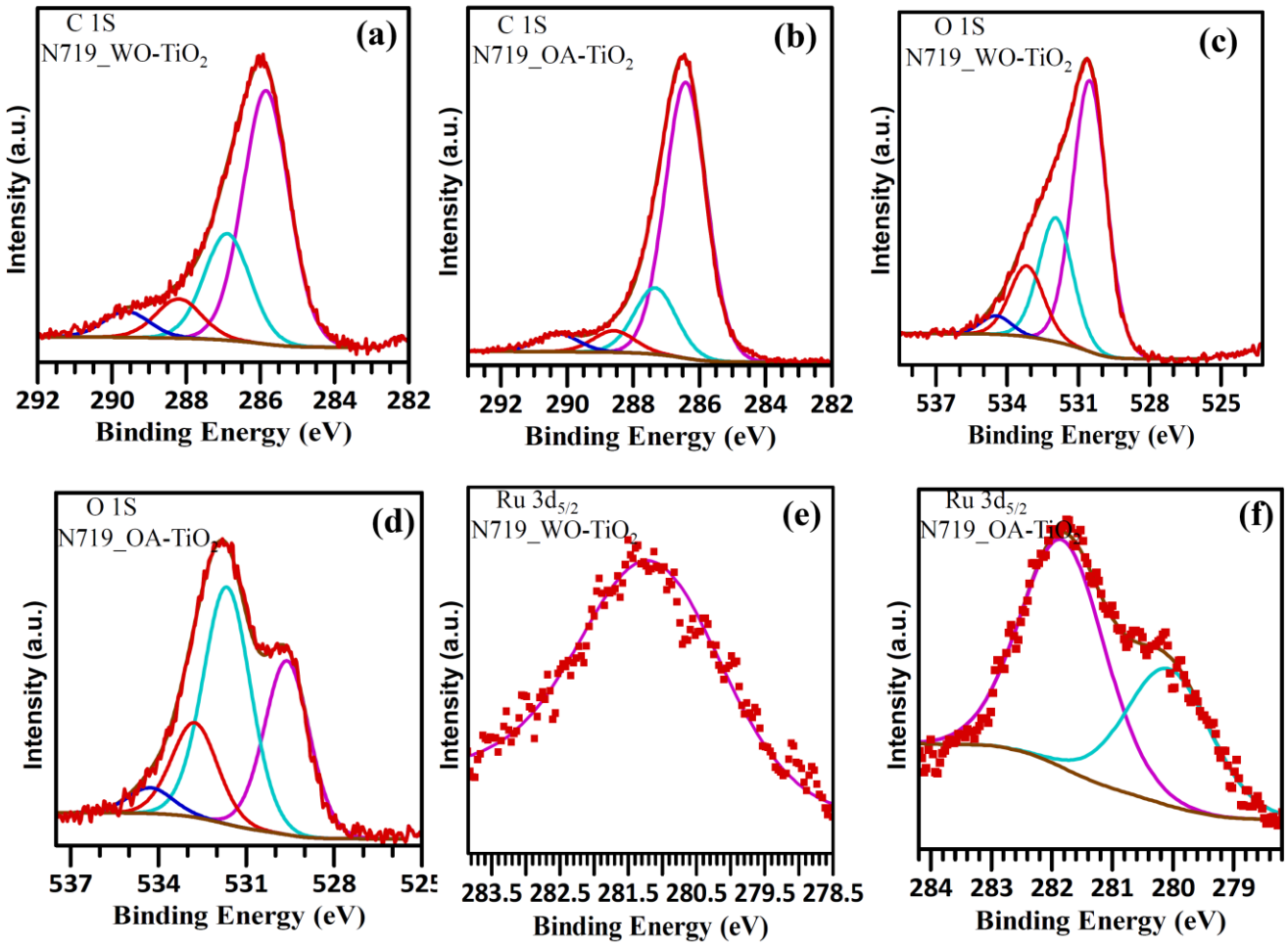
C 1S
N719_WO-TiO2
(a)
C 1S
N719_OA-TiO2
(b)
O 1S
N719_WO-TiO2
(c)
O 1S
N719_OA-TiO2
(d)
Ru 3d5/2
N719_WO-TiO2
(e)
Ru 3d5/2
N719_OA-TiO2
(f)
Intensity (a.u.)
Binding Energy (eV)

Fig.6

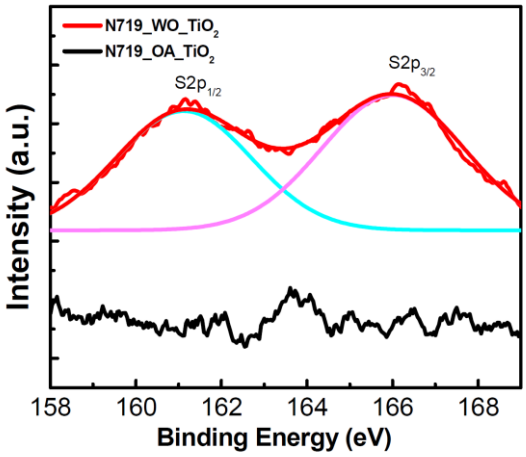
N719_WO_TiO2
N719_OA_TiO2
S2p1/2
S2p3/2
Intensity (a.u.)
158
160
162
164
166
168
Binding Energy (eV)

Fig.7

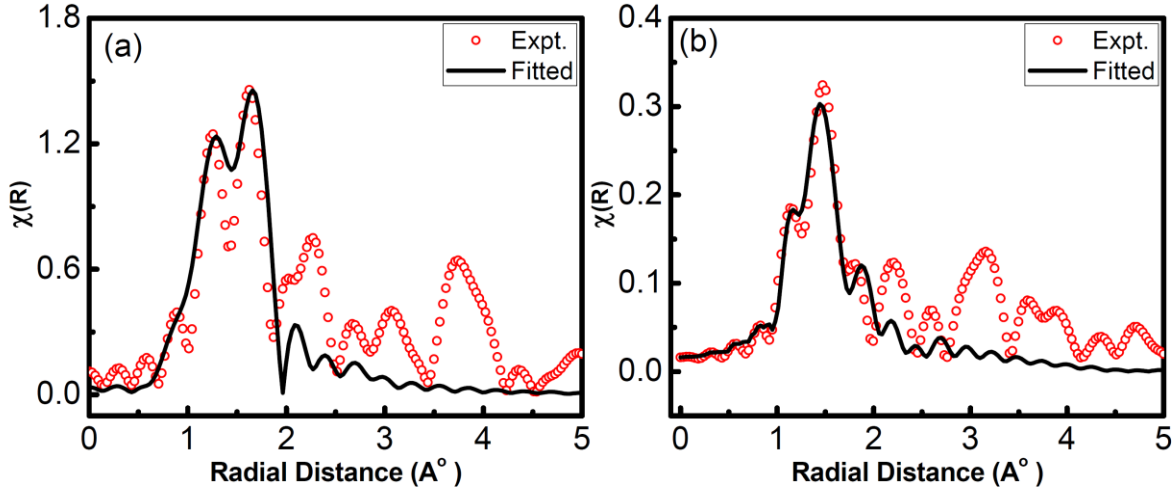
(a)
Expt.
Fitted
χ(R)
1.8
1.2
0.6
0.0
0
1
2
3
4
5
Radial Distance (A°)
(b)
Expt.
Fitted
χ(R)
0.4
0.3
0.2
0.1
0.0
0
1
2
3
4
5
Radial Distance (A°)

Fig.8

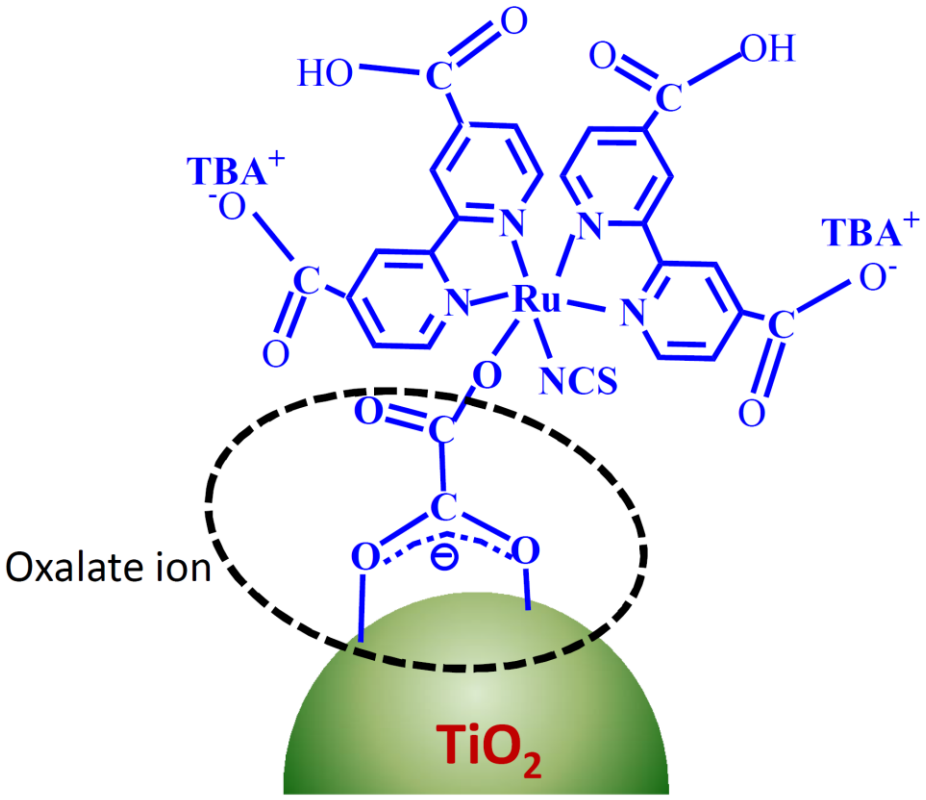
HO
O
C
O
OH
C
TBA+
-O
C
O
N
N
N
Ru
N
C
O
TBA+
O-
O
NCS
O
C
C
O
O
O
Oxalate ion
TiO2

Fig.9